KfK 3806
Dezember 1984

Matching Problems in Pulse Power Radial Transmission Lines

K. Mittag, A. Brandelik
Institut für Kernphysik

Kernforschungszentrum Karlsruhe

KERNFORSCHUNGSZENTRUM KARLSRUHE

Institut für Kernphysik

KfK 3806

Matching Problems in Pulse Power Radial Transmission Lines

K. Mittag, A. Brandelik

Kernforschungszentrum Karlsruhe GmbH, Karlsruhe

Kernforschungszentrum Karlsruhe GmbH
ISSN 0303-4003

Abstract

Matching Problems in Pulse Power Radial Transmission Lines

In this report we study the power transfer from a generator along a coaxial transmission line followed by a radial transmission line into a load, which in our application is a pseudo-spark plasma of about one millimeter diameter and about 15 cm in length. First the theoretical background based on transmission line theory is described. Then numerical results are presented. The main conclusion is that when matching the pulse power generator to the pseudo-spark plasma, the effect of the impedance transformation caused by the radial transmission line has to be taken into account. The conditions to obtain an optimal match are described.

Zusammenfassung

Anpassungsprobleme beim Transfer von gepulster Leistung über Radialleitungen

In diesem Bericht beschreiben wir den Leistungstransport von einem Generator über eine Koaxialleitung mit anschließender Radialleitung in eine Last, die für unsere Anwendung ein Pseudofunkenplasma von etwa ein Millimeter Durchmesser und etwa 15 cm Länge ist. Zunächst wird der theoretische Hintergrund erläutert, der auf der Leitungstheorie aufbaut. Dann werden die numerischen Ergebnisse dargestellt. Der wichtigste Schluß ist, daß bei der Anpassung eines Pulsleistungsgenerators an ein Pseudofunkenplasma die Impedanztransformation durch die Radialleitung berücksichtigt werden muß. Die Bedingungen, unter denen man optimale Anpassung erhält, werden beschrieben.

Contents

1. Introduction

In several applications, like z-pinch [1], plasma-focus [2], pseudo-spark [3] and ion beam diodes [4], a short pulse of high electromagnetic power has to be transferred from a generator via a transmission line to a load consisting of a high density plasma. Matching problems can occur if the pulse time is short or if the power has to be transferred into a very small volume. Techniques developed in microwave theory are appropriate to describe these phenomena, and to offer solutions in order to minimize mismatches.

In this report we study the power transfer from a generator along a coaxial transmission line followed by a radial transmission line into a load, which for our application is a pseudo-spark of about a millimeter diameter and about 15 cm in length. (Fig. 1) A radial transmission line simply consists of two parallel circular discs, in which the power flow is in the radial direction (from the outer radius to the inner one, in our case).

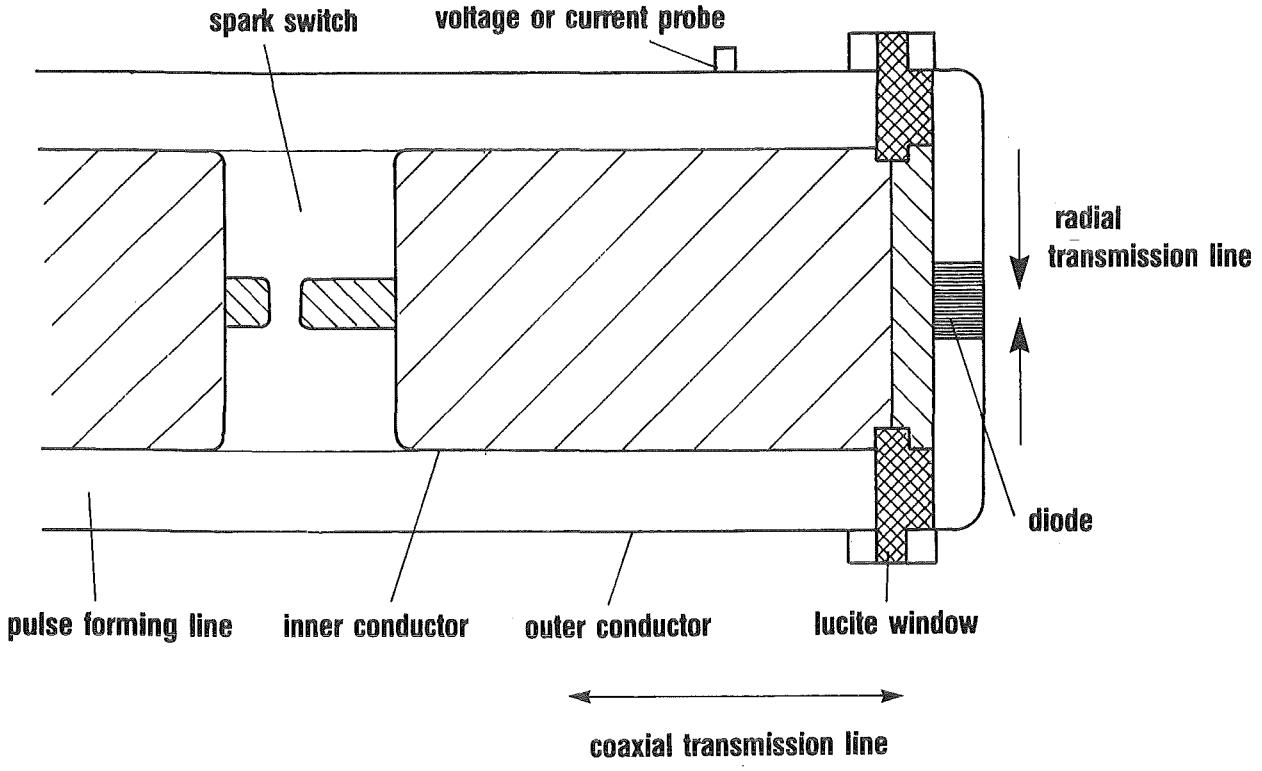

Fig. 1: Typical pulse power transmission line

The transfer properties for electromagnetic waves along the radial line are frequency dependent, whereas the coaxial line is non-dispersive. As a consequence, the effect of the radial line has to be taken into account in detail, if its radial extent is no longer much smaller than the wavelength.

In the case of our pseudo-spark diode the pulse duration is on the order of 100 ns. The transmission line is filled with water. Hence, the wavelength of the fundamental frequency component of the pulse is about 6.6 m, which still is large compared to the dimensions of our radial line (about 30 cm diameter). Therefore, no severe reflections are expected for the main part of the pulse, as long as the impedance of the load is matched to that of the coaxial transmission line. However, for the high frequency components of the pulse (like 50 MHz) distortions will occur.

The high power pulsed diodes can be classified into surface diodes and filament diodes. In the first class the electromagnetic wave energy is transferred to the plasma along a ring-shaped surface of some cm diameter. In the second class (z-pinch, pseudo-spark) this energy transfer occurs into a cylindrical filament having a length of some cm and a diameter ranging from mm to µm. It is of great interest how much the electromagnetic wave energy can be concentrated before conversion into kinetiv energy of the plasma. The radial line analysis gives an answer about the efficiency of this extreme energy compression.

Another application of this work will be in the evaluation of experiments. Voltage and current are measured with pick-ups as a function of time in the transmission line. Using these data and the transfer properties of the lines, the voltage and current can be calculated at the location of the diode.

2. Properties of transmission lines

2.1 From Maxwells equations to the principal transmission line modes

In this chapter we shall outline the theoretical background behind the formulas of the transmission line theory. [5,6,7,8] This will facilitate the discussion about the applicability of the theory and the importance of the approximations made. The macroscopic Maxwells equations form the basis for the following:

$$\begin{aligned} \operatorname{rot} \vec{E} &= -\frac{\partial}{\partial t}(\mu\vec{H}); \qquad \operatorname{div}(\varepsilon\vec{E}) = 0 \\ \operatorname{rot} \vec{H} &= \frac{\partial}{\partial t}(\varepsilon\vec{E}); \qquad \operatorname{div}(\mu\vec{H}) = 0 \end{aligned} \tag{1}$$

$\vec{E}$ and $\vec{H}$ are the electric and magnetic fields.

$\varepsilon = \varepsilon_r\varepsilon_0$; $\mu = \mu_r\mu_0$ are the (2)

total permittivity and permeability of the material filling the transmission line, now assumed to be space and time independent. The influence of free charges and currents inside this material is neglected. The boundary conditions at the metalic surfaces of the transmission lines are taken to be those of an ideal conductor, thus dissipative effects are neglected.

For any time dependence of an electromagnetic pulse one can make a Fourier analysis:

$$\vec{E}(t) = \frac{1}{2\pi} \int_{-\infty}^{\infty} \vec{E}_f(\omega)\, e^{j\omega t}\, d\omega \qquad (3)$$

with the complex Fourier transform $\vec{E}_f(\omega) = \int_{-\infty}^{\infty} \vec{E}(t)\, e^{-j\omega t}\, dt$, and (4)

similarly for the magnetic field.

Inserting this into (1) yields Maxwells equations for the Fourier transforms, that is for the frequency components

$$\vec{E}_f(\omega)\, e^{j\omega t} \quad \text{and} \quad \vec{H}_f(\omega)\, e^{j\omega t} \qquad (5)$$

of the pulse:

$$\begin{aligned} \text{rot}\ \vec{E}_f &= -j\omega\mu\vec{H}_f\ ; \quad \text{div}\ \vec{E}_f = 0 \\ \text{rot}\ \vec{H}_f &= j\omega\varepsilon\vec{E}_f\ ; \quad \text{div}\ \vec{H}_f = 0 \end{aligned} \qquad (6)$$

In the following we drop the subscripts f and ω for simplicity, and study the properties of a single Fourier components (equ. 5) only.

Combing equ. (6) one can uncouple the electric and magnetic fields, and obtains the wave equations:

$$\nabla^2\vec{E} + k^2\vec{E} = 0; \quad \nabla^2\vec{H} + k^2\vec{H} = 0 \qquad (7)$$

$$k^2 = \varepsilon\mu\omega^2 \qquad (8)$$

In case either the electric or the magnetic field is known, the other can be obtained from (1) by time integration.

In order to obtain solutions for the spatial dependence of the fields, the geometry of the boundary has to be specified. Analytical solutions can be obtained, if the geometry possesses some kind of symmetry. The symmetry properties of the coaxial and the radial line can be exploited most effectively in cylindrical coordinates r,ϕ,z, as shown in Figs. 2,3.

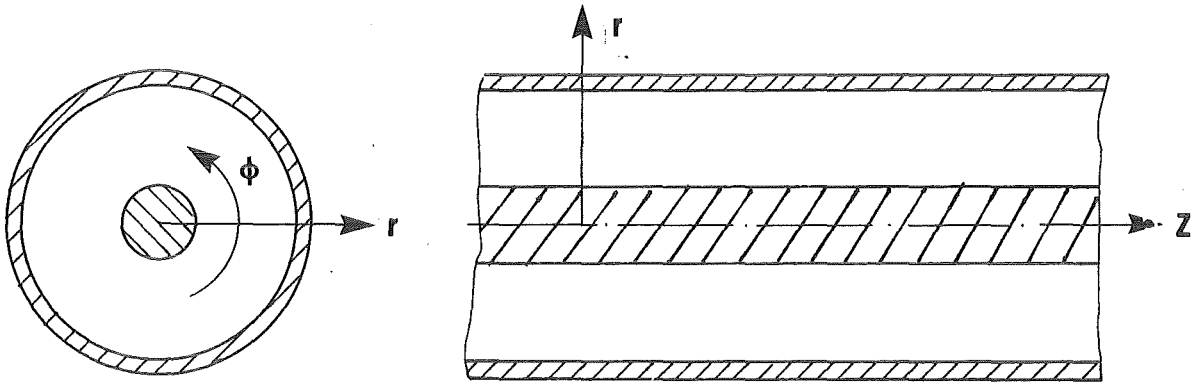

Fig. 2: Coordinates in coaxial line

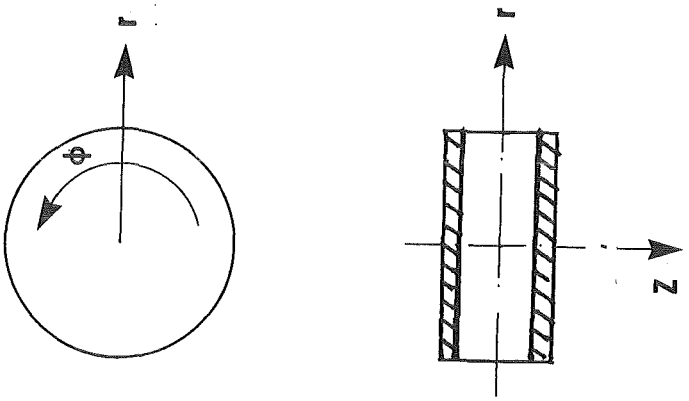

Fig. 3: Coordinates in radial line (left: top view, right side view)

In cylindrical coordinates equ. 6 look like:

$$\frac{1}{r}\frac{\partial E_z}{\partial \phi} - \frac{\partial E_\phi}{\partial z} = -j\omega\mu H_r, \qquad \frac{1}{r}\frac{\partial H_z}{\partial \phi} - \frac{\partial H_\phi}{\partial z} = j\omega\varepsilon E_r,$$

$$\frac{\partial E_r}{\partial z} - \frac{\partial E_z}{\partial r} = -j\omega\mu H_\phi, \qquad \frac{\partial H_r}{\partial z} - \frac{\partial H_z}{\partial r} = j\omega\varepsilon E_\phi, \qquad (9)$$

$$\frac{1}{r}\frac{\partial (rE_\phi)}{\partial r} - \frac{1}{r}\frac{\partial E_r}{\partial \phi} = -j\omega\mu H_z, \qquad \frac{1}{r}\frac{\partial (rH_\phi)}{\partial r} - \frac{1}{r}\frac{\partial H_r}{\partial \phi} = j\omega\varepsilon E_z.$$

The general solutions of these equations for the boundary conditions of Figs. 2,3 consists of series of characteristic modes: E-modes, and H-modes - which are derivable from a single component of E or H in the direction of propagation of the wave - or transverse electromagnetic TEM-modes, which only have field components perpendicular to the direction of propagation.

Now, we shall leave the general treatment, which can be carried through for more complicated pulse power transmission lines (see Fig. 1) only with involved computer codes. In the following, we neglect the influence of geometrical discontinuities like the spark switch or the lucite window. Also we shall neglect the excitation of higher order modes and shall take into account the fundamental modes only, both inside the coaxial and inside the radial line. This can be justified as follows. At the end of the charging up of the pulse forming line the field inside the line can be taken as stationary, that is purely electrostatic, having only radial electric field components.When the spark switch closes only those modes in the coaxial transmission line will be excited with large amplitudes, which couple well to this E_r-field and to the rotationally symmetric magnetic field H_ϕ caused by the current flowing now along the inner conductor of the coaxial transmission line. This turns out to be the single principal,rotationallysymmetric TEM-mode, having as non-vanishing field components only E_r and H_ϕ. In turn, the azimuthal magnetic field H_ϕ of this mode only couples well to the magnetic field H_ϕ of the principal mode of the radial transmission line (see Fig. 4). The transition region between coaxial and radial line can only be treated with complicated computer codes, and will be neglected in the following.

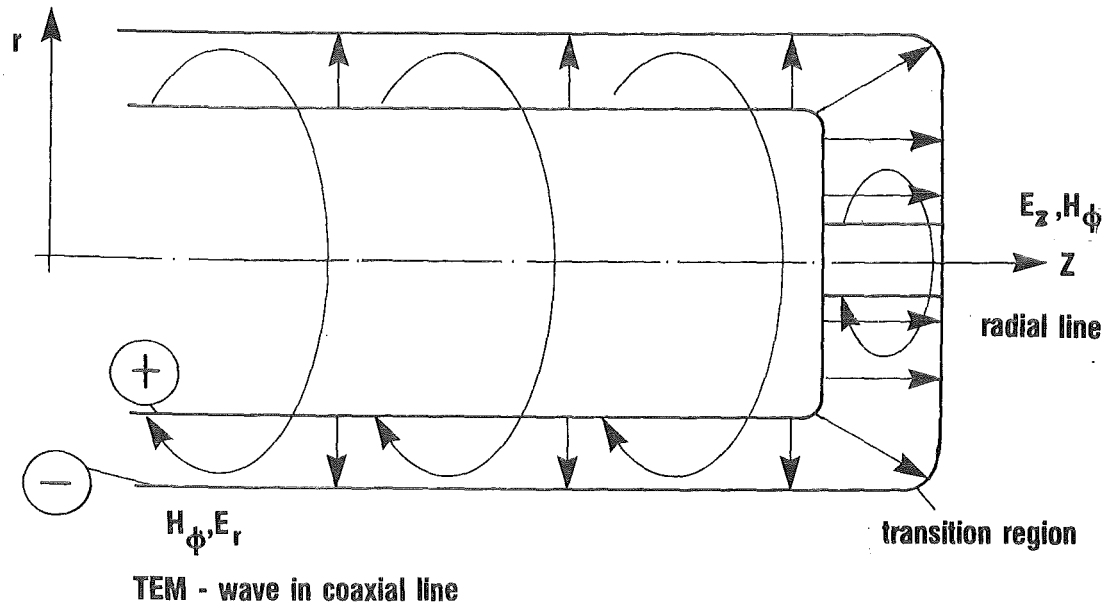

Fig. 4: Field configurations of the principal modes in the coaxial and radial transmission lines

2.2 The principal mode of the coaxial line

The principal mode of the coaxial line (see Fig. 4) is characterized by

$$H_r = H_z = 0 \quad \text{and} \quad E_\phi = E_z = 0. \tag{10}$$

From (7) follows the wave like behaviour in the z-direction:

$$\frac{\partial^2 H_\phi}{\partial z^2} + k^2 H_\phi = 0, \quad H_\phi(z) \sim e^{\pm jkz}, \tag{11}$$

and the transverse variation of the fields is according to (9):

$$\frac{\partial(rH_\phi)}{\partial r} = 0; \quad \frac{\partial E_r}{\partial \phi} = 0; \quad -\frac{\partial H_\phi}{\partial z} = j\omega\varepsilon E_r \tag{12}$$

Hence:

$$H_\phi(r,\phi,z,t) = \frac{I_o e^{j(\omega t \pm kz)}}{2\pi r} \tag{13}$$

$$E_r(r,\phi,z,t) = \mp \frac{I_o}{2\pi}\sqrt{\frac{\mu}{\varepsilon}}\,\frac{e^{j(\omega t \pm kz)}}{r},$$

where I_o is the total current flowing along the inner (or outer) conductor. The characteristic impedance of the coaxial line is defined as the ratio of voltage V between inner and outer conductor (radius a,b) to current:

$$Z_o = \frac{V}{I} = \frac{\int_a^b |E_r|\, dr}{I} = \frac{1}{2\pi}\sqrt{\frac{\mu}{\varepsilon}}\,\ln\frac{b}{a} \tag{14}$$

If I_+ is the current flowing in the positive z-direction, and I_- that flowing in the negative z-direction, the general solution can be written using equ. (13), (14) as:

$$\begin{aligned} I(z) &= (I_+ + I_-)\cos kz - j(I_+ - I_-)\sin kz \\ V(z) &= Z_o(I_+ - I_-)\cos kz - jZ_o(I_+ + I_-)\sin kz, \end{aligned} \tag{15}$$

where a time dependence $e^{j\omega t}$ is understood.

In case the voltage V_1 and the current I_1 are known at a position z_1, they can be calculated at any other position z from

$$V(z) = V_1\cos\psi + jZ_o I_1 \sin\psi; \qquad \psi = k(z_1 - z) \tag{16}$$

$$I(z) = I_1\cos\psi + j\frac{V_1}{Z_o}\sin\psi ,$$

which follows directly from equ. (15).

Most often, only the impedance Z = V/I is of importance, since in a wave both voltage and current scale with the same amplitude factor:

$$Z(z) = \frac{V(z)}{I(z)} = Z_o \cdot \frac{Z_1\cos\psi + jZ_o\sin\psi}{Z_o\cos\psi + jZ_1\sin\psi}; \quad Z_1 = \frac{V_1}{I_1} \tag{17}$$

2.3 The principal mode of the radial line

This mode also only has two non-vanishing field components, namely E_z and H_ϕ, whereas

$$H_z = H_r = 0 \quad 0; \quad E_\phi = E_r = 0 \tag{18}$$

From equ. (9) follows:

$$\frac{\partial E_z}{\partial \phi} = 0; \quad \frac{\partial H_\phi}{\partial z} = 0; \quad H_\phi = \frac{1}{j\omega\mu}\frac{\partial E_z}{\partial r}, \text{ and from (7):} \tag{19}$$

$$\frac{r^2\partial^2 E_z}{\partial r^2} + r\frac{\partial E_z}{\partial r} + k^2 r^2 E_z = 0 \tag{20}$$

The solution of (20) are the Bessel functions of the first kind of order 0, J_o and Y_o.

As for the coaxial line (equ. 13), also for the radial line the fields can be written as travelling waves (+ sign: travels radially inward)

$$E_z = \frac{V_o}{b}\,[J_o(kr) \pm jY_o(kr)]\,e^{j\omega t} \tag{21}$$

$$H_\phi = j\sqrt{\frac{\varepsilon}{\mu}}\,\frac{V_o}{b}\,[J_1(kr) \pm jY_1(kr)]\,e^{j\omega t}$$

b is the distance between the discs of the radial line and V_o the voltage amplitude. The general solution written in the standing wave form with the time dependence $e^{j\omega t}$ understood then can be written with complex constants A,B as:

$$V(r) = AJ_0(kr) + BY_0(kr)$$
$$jZ_0(r)I(r) = AJ_1(kr) + BY_1(kr) \qquad (22)$$

with the characteristic impedance

$$Z_0(r) = \sqrt{\frac{\mu}{\epsilon}}\,\frac{b}{2\pi r}\,, \qquad (23)$$

the total current $I(r) = -2\pi r\, H_\phi(r)$, and the voltage $V(r) = E_z(r)\cdot b$ (the sign convention is chosen such that a positive current flows radially outward). Again, voltage and current at any position r can be calculated if they are known at other positions, e.g. $V_1 = V(r_1)$ and $I_2 = I(r_2)$.

If one defines:

$$C(r_1,r_2) = J_1(kr_2)Y_0(kr_1) - Y_1(kr_2)J_0(kr_1) \quad \left[\text{hence } C(r,r) = 2/(\pi kr)\right]$$
$$c(r_1,r_2) = Y_0(kr_2)J_1(kr_1) - J_0(kr_2)Y_1(kr_1) \qquad (24)$$

$$S(r_1,r_2) = Y_1(kr_2)J_1(kr_1) - J_1(kr_2)Y_1(kr_1)$$
$$s(r_1,r_2) = Y_0(kr_2)J_0(kr_1) - J_0(kr_2)Y_0(kr_1) \qquad (25)$$

Then:

$$V(r) = [V_1 C(r,r_2) + jZ_0(r_2)\, I_2\, s(r,r_1)]/C(r_1,r_2)$$
$$Z_0(r)I(r) = [Z_0(r_2)I_2\, c(r,r_1) + jV_1 S(r,r_2)]\,/C(r_1,r_2) \qquad (26)$$

From equ. (26) immediately follows how the impedance Z changes along the radial line from a radius r_1 to a radius r:

$$Z(r) = \frac{V(r)}{I(r)}\,;\quad \frac{Z(r)}{Z_0(r)} = \frac{Z(r_1)C(r,r_1)+jZ_0(r_1)s(r,r_1)}{Z_0(r_1)c(r,r_1)+jZ(r_1)S(r,r_1)} \qquad (27)$$

This is formally rather similar to the transfer properties of the coaxial line (equ.17). However, for the coaxial line the impedance Z is independent of z, if Z_1 is chosen to be equal to Z_0. For the radial line the impedance Z(r) always depends on the radius r, since $C \neq c$ and $S \neq s$.

The time averaged power flow along the radial line can be calculated from the Poynting vector:

$$\vec{S} = \frac{1}{2}\,\mathrm{Re}(\vec{E} \times \vec{H}^*) = -\frac{1}{2}\,\mathrm{Re}(E_z\, H_\phi^*)\,\vec{e} \qquad (28)$$

In case there is a wave of voltage amplitude V_+ travelling radially outward, and another one of amplitude V_- travelling radially inward the result is:

$$S = \sqrt{\frac{\varepsilon}{\mu}} \frac{V_+^2 - V_-^2}{\pi k r b^2} \tag{29}$$

Then the total power flowing through the cylinder surface at a radius r is

$$\int_0^{2\pi} \int_0^b S\, r\, dz\, d\phi = 2 \sqrt{\frac{\varepsilon}{\mu}} \frac{V_+^2 - V_-^2}{kb}, \tag{30}$$

which is independent of r. This means, that in a homogeneous radial line the waves given by equ. 21 travel without reflection, although the ratio of electric to magnetic field or the impedance does change.

2.4 Impedance of the radial line at very small radius

The characteristic impedance of the radial line scales as 1/r (23). At first glance this suggests that it would be very difficult to transfer power to a load located at a very small radius. However, when analyzing the problem more carefully, one has to study how the total impedance Z(r) scales as a function of the radius r. If the impedance at the outer radius r_1 is known, from equ. (27,24,25) one obtains in the limit of very small radius r:

$$Z(r) \underset{r\to 0}{=} -j \sqrt{\frac{\mu}{\varepsilon}} \frac{kb}{2\pi} \ln(kr) \tag{27a}$$

Thus the radial line impedance only has a logarithmic singularity at r=0. Matching a low impedance load located at a very small radius to a radial transmission line will not be possible without reflections. However, the amount of reflections might be tolerable as long as power efficiency aspects do not play a dominant role.

3. Matching a pulse power transmission line to the load

The next step is to represent the pulse power transmission line of Fig. 1, 2 by a simple network. In this concept, the transition region between coaxial and radial line is neglected. We assume, that the total current flowing e.g. on the inner conductor of the coaxial line continues to flow radially on the radial line. Similarly, we assume that the voltage matches continuously from the coaxial to the radial line. In a similar manner discontinuities along the coaxial or the radial lines can be treated, e.g. if the dielectric changes its ε from water to air.

Consider the following example in Fig. 5.

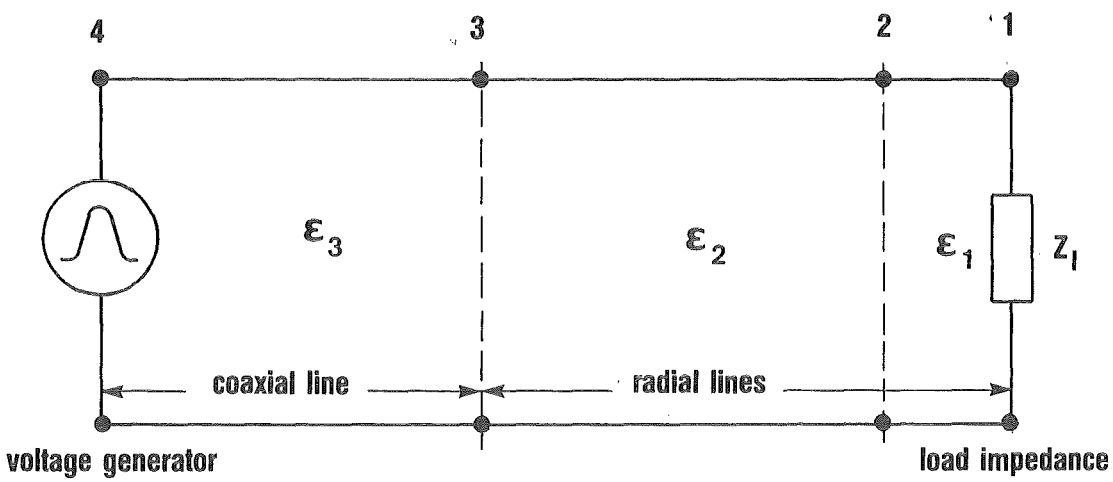

Fig. 5: Network representing the pulse power transmission lines of Fig. 1,2; ε = dielectric constant; voltage generator, coaxial and radial lines are assumed to be lossless.

In this case we assume that the load impedance is known at position 1 (e.g. at the inner bore radius of a pseudo spark chamber) for a certain frequency or as a function of frequency. Then using equ. (27) and equ. (17) the impedance Z at the position 4 (voltage generator or measuring probe) can also be calculated for a certain frequency or as a function of frequency.

From general transmission line theory the ratio of the power incident (P_i) at position 4 to that reflected (P_r) due to the impedance mismatch is given for a fixed frequency by:

$$\frac{P_r}{P_i} = \left|\frac{Z-Z_o}{Z+Z_o}\right|^2 , \quad \text{with } Z = \text{load impedance as caluclated e.g. at position 4, and} \tag{31}$$

Z_o = characteristic impedance of the coaxial line.

In general, the voltage measured at position 4 can be fitted quite well to a $\sin^2$ - function:

$$V(t) \approx \begin{cases} V_o \sin^2 \Omega t & \text{for } 0 \leq t \leq T \quad ; \quad \Omega = \pi/T \\ o & \text{else} \end{cases} \tag{32}$$

This function can readily be Fourier - analyzed :

$$V(t) = \frac{V_o \cdot T}{2\pi} \int_0^\infty [\ ]\ d\omega \qquad (33)$$

$$[\ ] = \{\cos\omega t\ \sin\omega T + \sin\omega t\ (1-\cos\omega T)\} \cdot \cdot \left\{ \frac{1}{\omega T} + \frac{1}{2(2\pi-\omega T)} - \frac{1}{2(2\pi+\omega T)} \right\}$$

Since now for each frequency the impedance $Z(\omega)$ is known at position 4, also the corresponding current can be calculated:

$$I(\omega) = V(\omega)/Z(\omega) \qquad (34)$$

Then according to equ. 16 and 26 the voltage and current can be calculated along the transmission line for each frequency. Finally, these are summed up again to yield the voltage and current as a function of time at any position along the line.

Now for a given pulse power transmission line one can vary the load impedance in order to find its optimum value to minimize mismatches. This in turn might be used to optimize the diode (load) design such, that most of the incident power is transferred to the diode. In case the diode impedance is known, from the voltage estimated or measured at position 4 the voltage and current at the diode can be predicted.

Another application of the methods described above would be to start from the measured voltage $V(r_1,t)$ and current $I(r_2,t)$ signals, obtained at positions r_1 and r_2 as a function of time. These can be Fourier-analyzed numerically, and thus voltage and current at the position of the diode can be calculated. This method will be more accurate then that using simple lumped circuit theory, describing the lines by a few capacitances and inductances.

4. Pulse power transfer along a transmission line to a pseudo-spark pinch - Numerical results -

4.1 The reference geometry

The calculations to be discussed below were done for the reference geometry shown in Fig. 6. The voltage generator is located at the open end of the 3 Ohm-coaxial line and delivers a pulse

$$V(t) = \begin{cases} (\sin^2 \frac{\pi t}{T}) \cdot \text{Volt} & \text{for } 0 \leq t \leq T = 100 \text{ ns} \\ 0 & \text{else} \end{cases}$$

In the calculations this pulse is followed along the line both as a function of time and of space. The length of the coaxial line was chosen such that the pulse travel time from the generator to the load is 110 ns. The load is assumed to be localized at a diameter of 3 mm in the pseudo-spark diode.

The transition region between the coaxial and the radial line is neglected in the calculations.

4.2 Reflections along the line

In Fig. 7 the travel time of the pulse from the generator to the load was 150 ns. The load impedance was real and its value 4 Ohm. All graphs are plotted as a function of time. Voltage, current and power is evaluated at four positions along the line (refer to Fig. 6 for identification). The sign convention was chosen such that a negative power means power flow from the generator to the load, that is radially inward along the radial line.

The $\sin^2 \pi t/T$ - voltage pulse (4) at the generator is easily identified. The corresponding current and power pulses between 0 and 100 ns correspond directly to the 3 Ohm impedance of the coaxial line.

Since the coaxial line is not perfectly matched to the radial one, and further there are impedance mismatches due to transitions in gap spacing and in the dielectric constant ε, and also the load also is not perfectly matched to the radial line, there occur wave reflections because of these impedance mismatches. The main reflection occurs at the load. The corresponding current pulse arrives back at the generator after 300 ns total travel time. Clearly, at that time the voltage at the generator position remains zero, since this is required from the input

data. All of the power arriving at the generator is reflected (power travelling outward equals that travelling inward, the sum is zero), and then travels back again towards the load. All of the power losses occur at the load, because generator and lines were assumed to be lossless in this model.

Comparing the voltage and current at the four positions along the line, it is clear that the transformations caused by the radial line have a large influence on the power transfer. Notice especially the voltage enhancement of about 1.5 at the transition from coaxial to radial line (3).

4.3 Matching the load to the transmission lines

Fig. 8 shows the main pulse at the position of the load for various load impedances which are assumed to be purely ohmic. The best power match between load and transmission lines is achieved if the load impedance is about 5 Ohm. For this case 27% of the incident power is reflected due to the impedance mismatch. This value is obtained by integrating the power in Fig. 8 as a function of time and then comparing this result to the power delivered from the generator. In case of a 3 Ohm load impedance, the reflected power increases to 30%. The effect of the impedance transformation of the radial line is clearly demonstrated, since otherwise there would be a perfect match without any reflections for a 3 Ohm load connected to a 3 Ohm transmission line. The ratio of reflected power to incident power evaluated from Fig. 8 is plotted as a function of the load impedance in Fig. 9 (single circles).

This ratio was calculated also for a fixed frequency of 5 MHz, which is about the main Fourier-component in the 100 ns - pulse. The results are shown in Fig. 9 by the solid curves. Parameter of these curves is the imaginary part of the impedance (the sign convention of the impedance corresponds to that of the power flow; a negative imaginary part corresponds to inductive loading, a positive one to capacitive loading). There is very good agreement between the results obtained from the pulse calculations and those obtained for 5 MHz fixed frequency (compare single circles with curve labeled 0). The conclusion is that indeed most of the properties of the power transfer from generator to load can be estimated from the properties of the main Fourier component of the pulse.

The dielectric constant of the diode material (between positions (1) and (2) in Fig. 6)was changed for the 5 MHz, fixed frequency calculation between $\varepsilon_r = 1$ and $\varepsilon_r = 81$. This causes changes of less then 0.1% in the reflected power, as is expected from the relation between wavelength (60 m and 6.6 m) to diode radius (2.5 cm).

The ratio of reflected to incident power was calculated also for the fixed frequency of 50 MHz (Fig. 10). In this case for a purely ohmic load of more then 8 Ohm over 90% of the incoming power is reflected.

From Fig. 9 one can conclude, that an optimal match between transmission lines and load should be obtained for a load having about an impedance of (- 3,5) Ohm at 5 MHz. This was modelled by a capacity of - 4.7 nF shunted to a real resistance of - 11 Ohm at the position of the load (r = 1.5 mm!). The result of the corresponding pulse transformation at the load position is shown in Fig. 11 (curve "radial, (-3,5)"), which for comparison also shows the pulse for a purely ohmic load of 3 Ohms (curve "radial (-3,0)"). Also given is the case of no radial line assuming only a coaxial line of 3 Ohms and a load of 3 Ohms (curve "coaxial" (-3,0)). For this latter case the pulse is transformed unchanged with no reflections from the generator to the load, as is expected from theory. The transformation caused by the radial line broadens the pulse and yields an asymmetric pulse shape; further the pulse rise time is decreased. Compared to this latter case the capacitive shunt causes a voltage enhancement of about a factor of two across the load. About 83% of the power is either dissipated in the 11 Ohm resistance or stored in the 4.7 nF capacitance until the time "204 ns". Thereafter about 13% of the power is again reflected back towards the generator.

Fig. 12 shows the case of a large mismatch which for the pseudo-spark chamber would be relevant before the plasma channel is established. The voltage is enhanced by a factor of 2 compared to that at the generator, which is typical for a standing wave pattern.

The curves in Fig. 13 were calculated for a real part of the impedance of -3 Ohm. The imaginary part of the impedance was varied. Comparing to the curve for zero imaginary part, it is evident, that an additional inductive loading in series to the ohmic load increases the mismatch, as is expected from Fig. 9. The current is delayed with respect to the voltage. It has been estimated, that a pinched plasma of 1.5 mm radius and 10 cm length would represent an inductance of about 78 nH. For this case 44% of the incident power is reflected. On the contrary an additional capacitive loading in series to the ohmic load (at the position of the load!) would improve the match. In this calculation it was assumed that this reactive load scales proportional to the frequency (curve "+160nH") and at 5 MHz it has a reactance of (-3,5) Ohm. Probably this cannot be realized technically. Nevertheless this case is reported, since it would yield the best obtainable match with all of the incident power absorbed in the load after the time "200 ns".

Next in Fig. 14 the position of the load is chosen to be at an even smaller radius on the radial line, namely at 0.15 mm. The reference curve for the load at 1.5 mm with (-3,0) - load is also shown. Going to the smaller radius the fraction of reflected power increases from 30% to 43% for a purely ohmic load. A pinch of 0.15 mm radius and 10 cm length has about an internal inductance of 120 nH, which was assumed to be in series to the -3 Ohm real part of the load for the other curve shown. For this case the fraction of reflected power is 57%.

Finally, also the pulse duration was varied. In order to study the influence of the high frequency components a pulse duration of 10 ns was chosen. Two curves are shown (Fig. 15), for a (-3,0) Ohm load, and for a (-3,0) Ohm load with a -78 nH series inductance. The pulse travel time along the line from generator to load was taken to be 11 ns. Only 9,4% of the incoming power is absorbed in the purely ohmic load in the main pulse until the time "22 ns". In the case of the additional series inductive load of -78 nH the match is improved such that now 15% of the power is absorbed until the time "18 ns" . Clearly, for the high frequency components the influence of the impedance transformation caused by the radial line becomes very large. This is because the extent of the radial line (15 cm) is comparable to the wave length (67 cm) of the main Fourier - component of the pulse 50 MHz (see also Fig. 10).

5. Conclusions

The pulse power transfer from a generator to a load along a coaxial line followed by a radial line was described using transmission line theory. A pulse having a $\sin^2 \pi t/T$ - shape at the generator was traced numerically both as a function of time and of space as it travels from the generator to the load. From the results it can be concluded that

1) The impedance transformation caused by the radial line cannot be neglected when searching for an optimal match between a generator and a pseudo-spark diode. A voltage enhancement of a factor 1.5 can occur at the transition from coaxial to radial line (Fig. 7).
2) For the reference geometry (Fig. 6, 3 Ohm coaxial line) and a purely ohmic load the optimal match is achieved with a 5 Ohm diode, causing still 27% of power reflection (Fig. 8, Fig. 9, pulse width = 100 ns).
3) The match can apparently be improved by shunting a 4.7 nF capacitance parallel to a 11 Ohm diode (at the position of the load, that is at 1.5 mm radius!) (Fig. 11). By this means the voltage across the load is enhanced about a factor

of 1.5 compared to the voltage at the generator. About 70% of the incident power is absorbed in the resistance, 13% is temporarely stored in the capacitance and then reflected back towards the generator.

4) A nearly perfect match could be achieved if an impedance of $(-3+j\frac{5 \cdot f}{5MHz})$ Ohm could be realized for the load (f = frequency).
5) The pulse power transfer for the 100 ns pulse width and the reference geometry (Fig. 6)is well described by the properties of the dominant 5 MHz-Fourier component, since its wavelength of 6.6 m is still large compared to the 15 cm extent of the radial line (Fig. 9).
6) In the case of an ohmic or capacitive load the pulse shape is broadened, the pulse rise time decreased, and the decay is longer than the built-up. (Fig. 11).
7) In the case of a large mismatch between generator and load the voltage is enhanced by a factor of 2 at the load (Fig. 12).
8) An additional series inductance to an ohmic load (as is inherent in a pinched plasma) deteriorates the match (Fig. 13). The current is delayed with respect to the voltage; the shape of the power pulse at the load deviates not much of that at the generator.
9) If the pinch radius decreases from 1.5 mm to 0.15 mm for an ohmic 3 Ohm load, the fraction of reflected power increases from 30% to 43% (Fig. 14). Taking the estimated inherent inductance of the 0.15 mm pinch into account (-160nH) this value is 57%. Thus it is clearly shown, that a large fraction of the incident power can indeed be transferred to a pinched plasma of very small radius located on the axis of a radial transmission line. This statement corresponds to the results of the theory that the total impedance of the radial line only has a logarithmic singularity on the axis (Chapter 2.4).
10) The high frequency components of the pulse (e.g. 50 MHz) are mostly reflected at the load (Fig. 10, Fig. 15).

The numerical results are summarized in Table 1.

TABLE 1

Summary of results from pulse power transformation along a coaxial and a radial line to a pseudo-spark diode

reflected power / incident power	real part of load impedance at 5 MHz (Ohm)	imaginary part of load impedance at 5 MHz (Ohm)	series inductance (nH)	parallel capacitance (nF)	load at radius (mm)	pulse duration (ns)	see figure 6
0.99	-1000	0	0	0	1.5	100	12
0.27	-5	0	0	0	1.5	100	8,9
0.30	-3	0	0	0	1.5	100	8,9
0.30	-3	+5	0	-4.7	1.5	100	11
0	-3	+5	"+160"	0	1.5	100	13
0.44	-3	-2.5	-78	0	1.5	100	13
0.54	-3	-5	-160	0	1.5	100	13
0.43	-3	0	0	0	0.15	100	14
0.57	-3	-3.7	-120	0	0.15	100	14
0.90	-3	0	0	0	1.5	10	15
0.85	-3	-2.5	-78	0	1.5	10	15

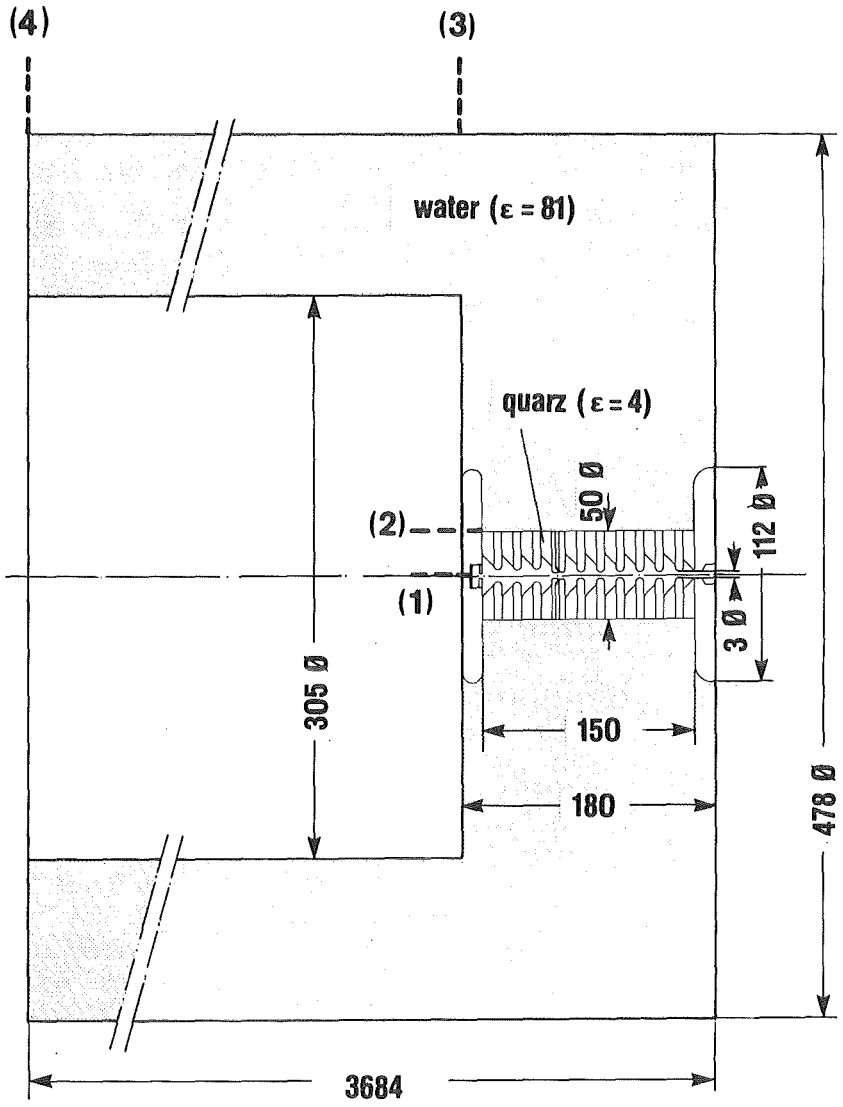

Fig. 6: Reference geometry for the calculations

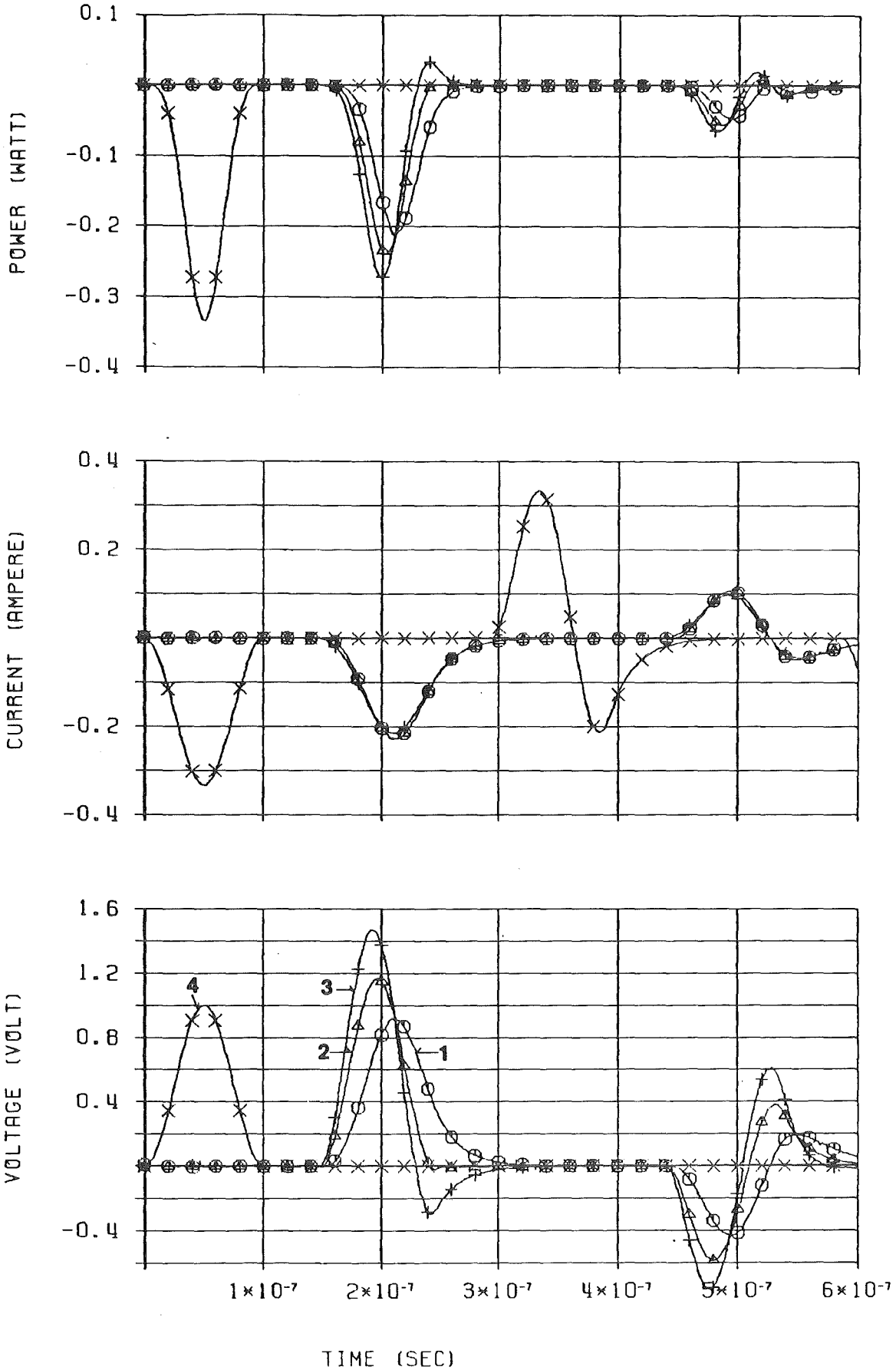

Fig. 7: Pulse travelling from the generator (4) along a coaxial line to a radial line (3), next to the pseudo-spark diode in the radial line (2), and finally to the pinched plasma (1); pulse travel time = 150ns; 4 Ohm load

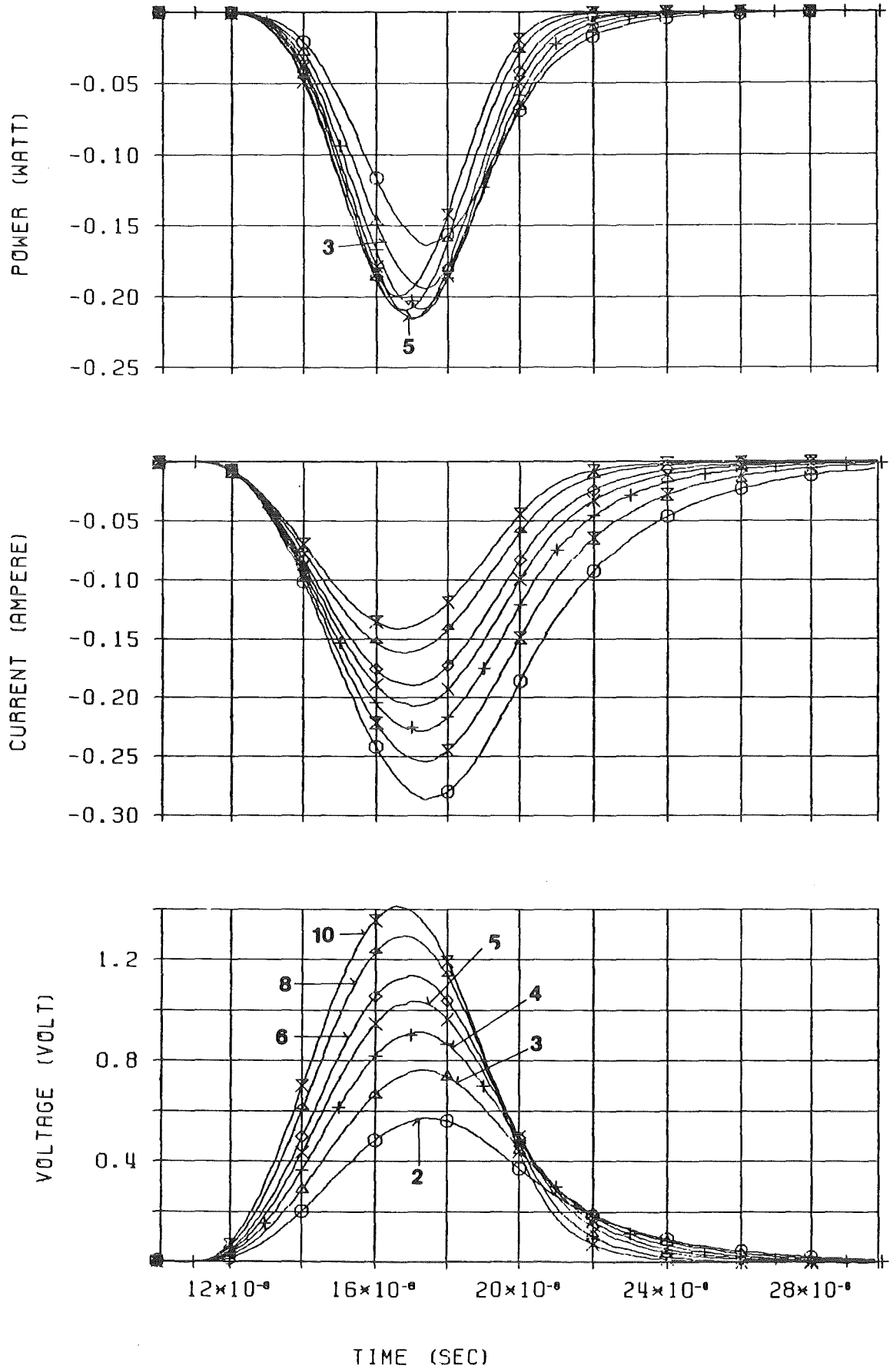

Fig. 8: Pulse at the position of the load for various purely ohmic load impedances; parameter is the load impedance in Ohm

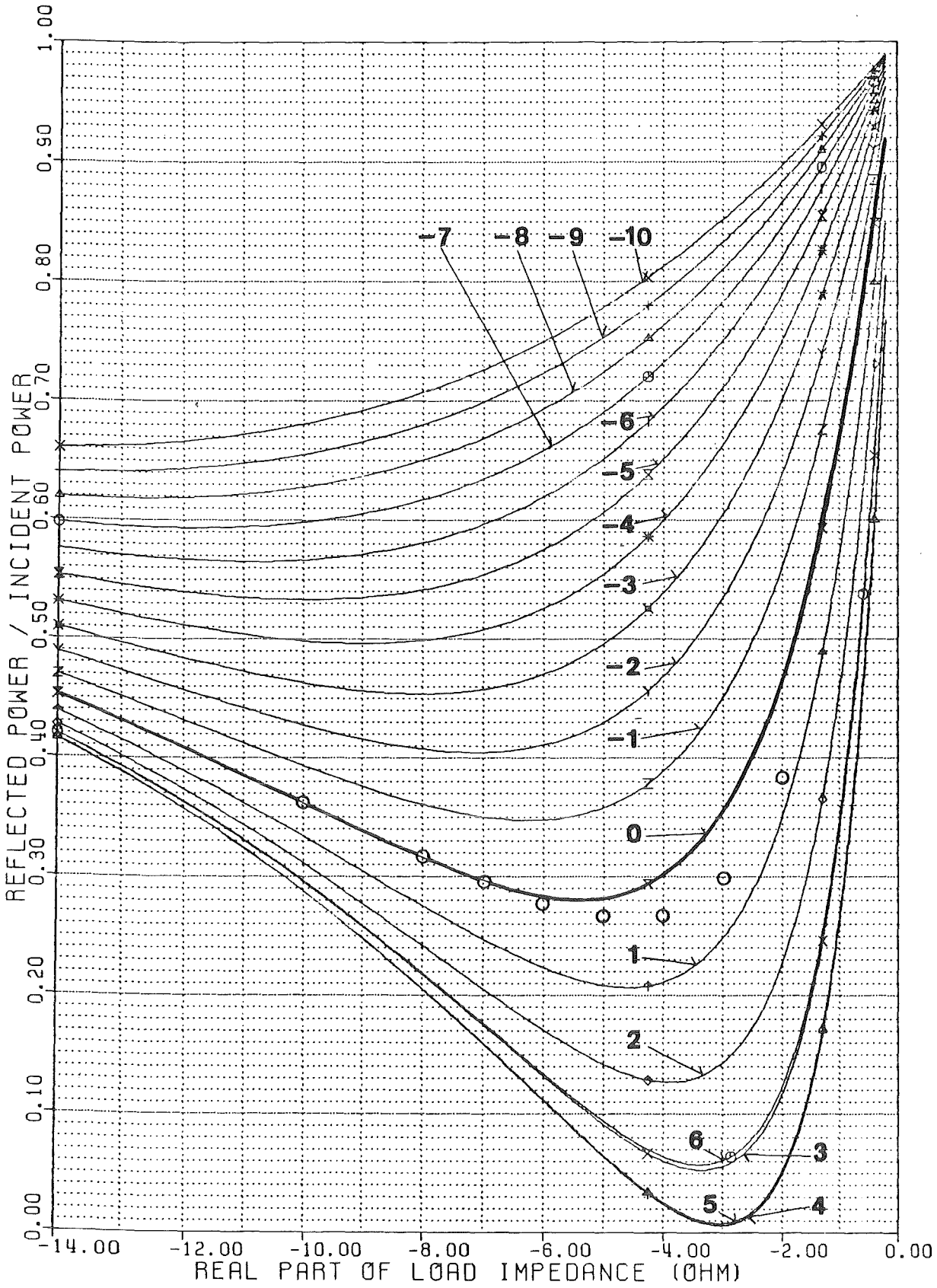

Fig. 9: Ratio of reflected to incident power as a function of the real part of the load impedance for a fixed 5 MHz frequency. Parameter is the imaginary part of the load in Ohm. Single circles were obtained from pulse calculations with a purely ohmic load.

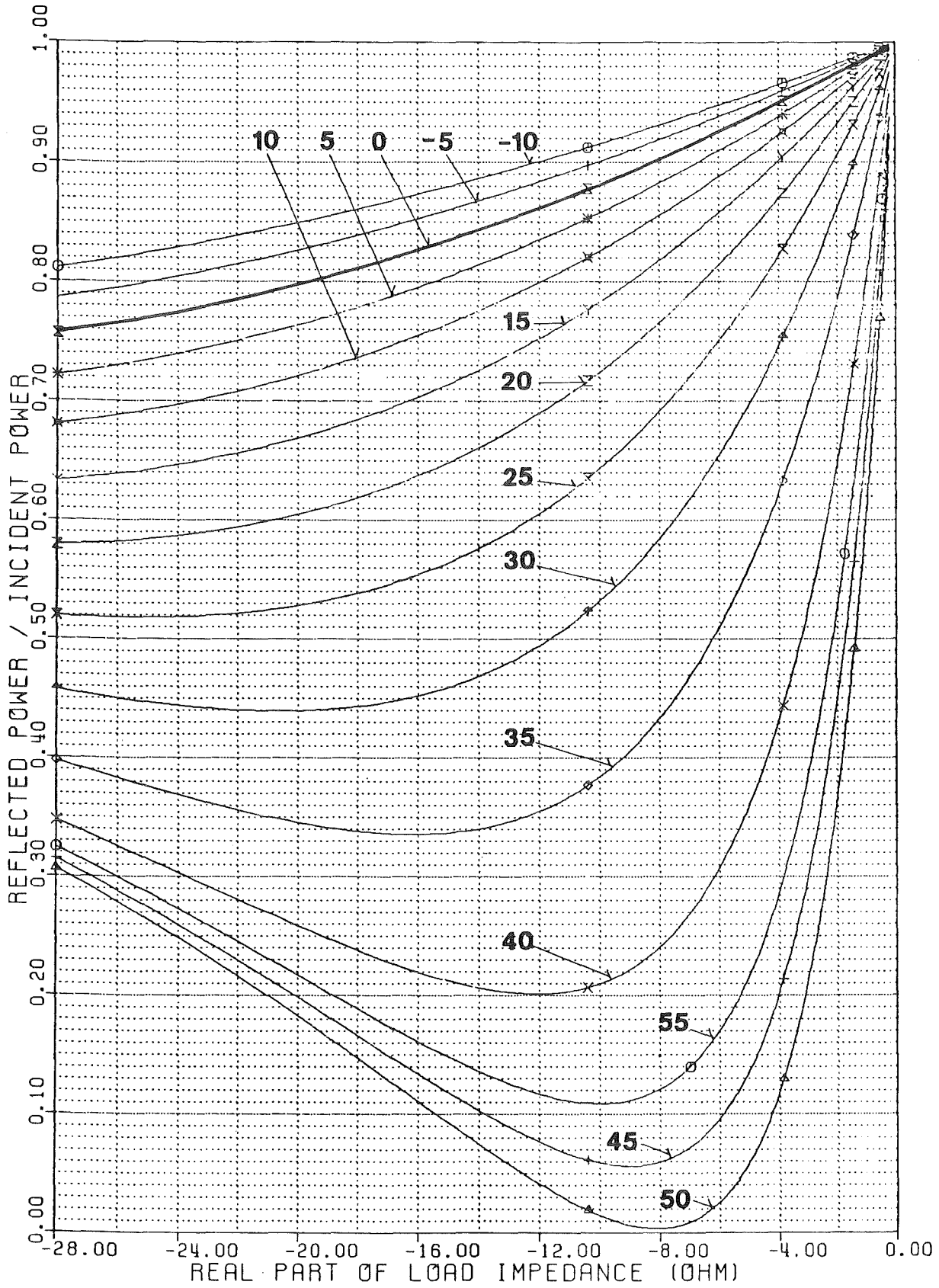

Fig. 10: Ratio of reflected to incident power as a function of the real part of the load impedance for a fixed 50 MHz frequency. Parameter is the imaginary part of the load in Ohm.

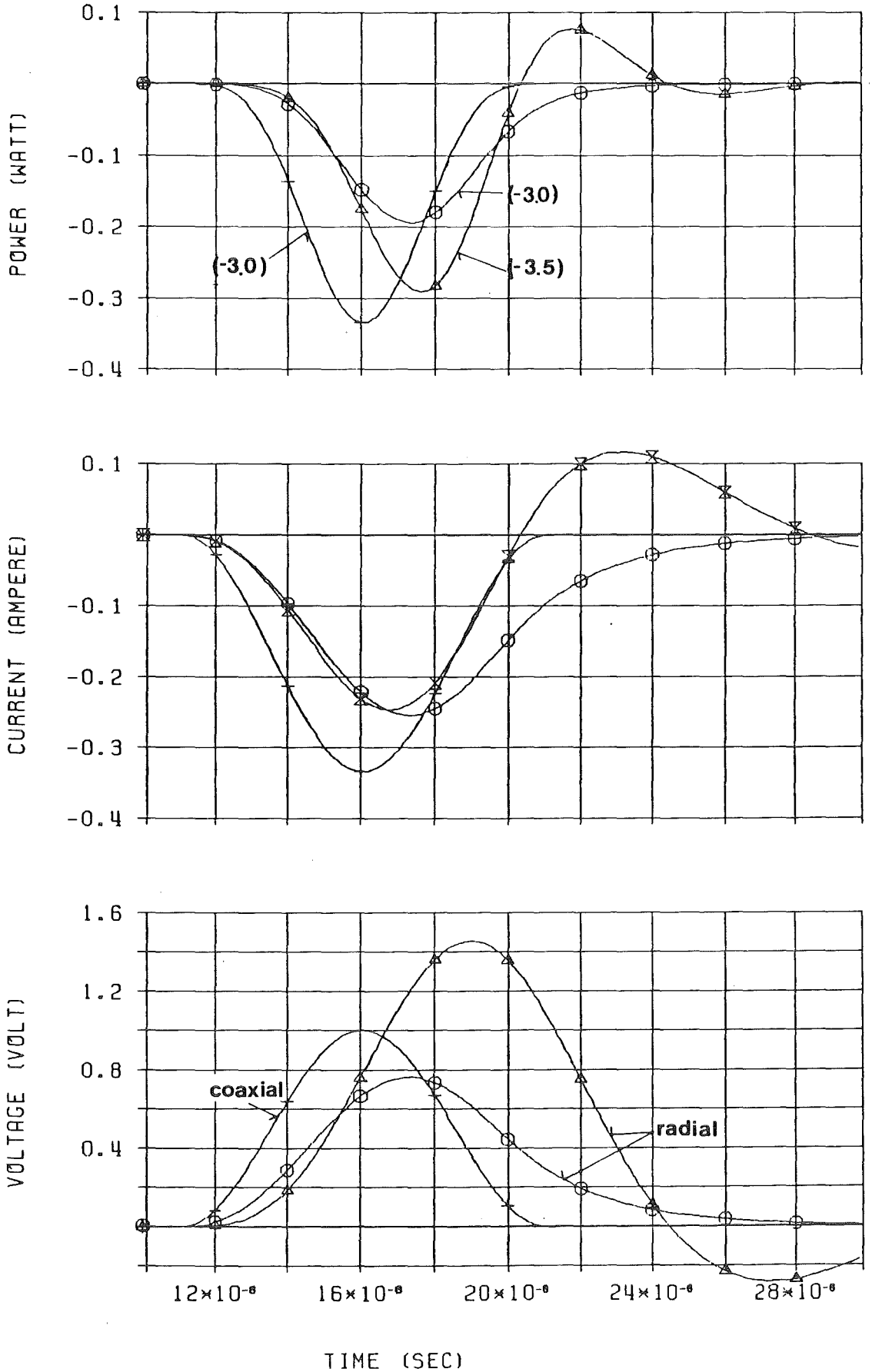

Fig. 11: Pulses at the load position, radius 1.5 mm. The generator pulse travels unchanged along a coaxial line (curve "coaxial"). The transformation caused by the radial line is evident from the curves "radial"). (-3,0) refers to a purely ohmic load of 3 Ohm. The curves (-3,5) are obtained when shunting a -4.7 nF capacity parallel to a -11 Ohm resistance at the load position, yielding a (-3,5) Ohm impedance at 5 MHz.

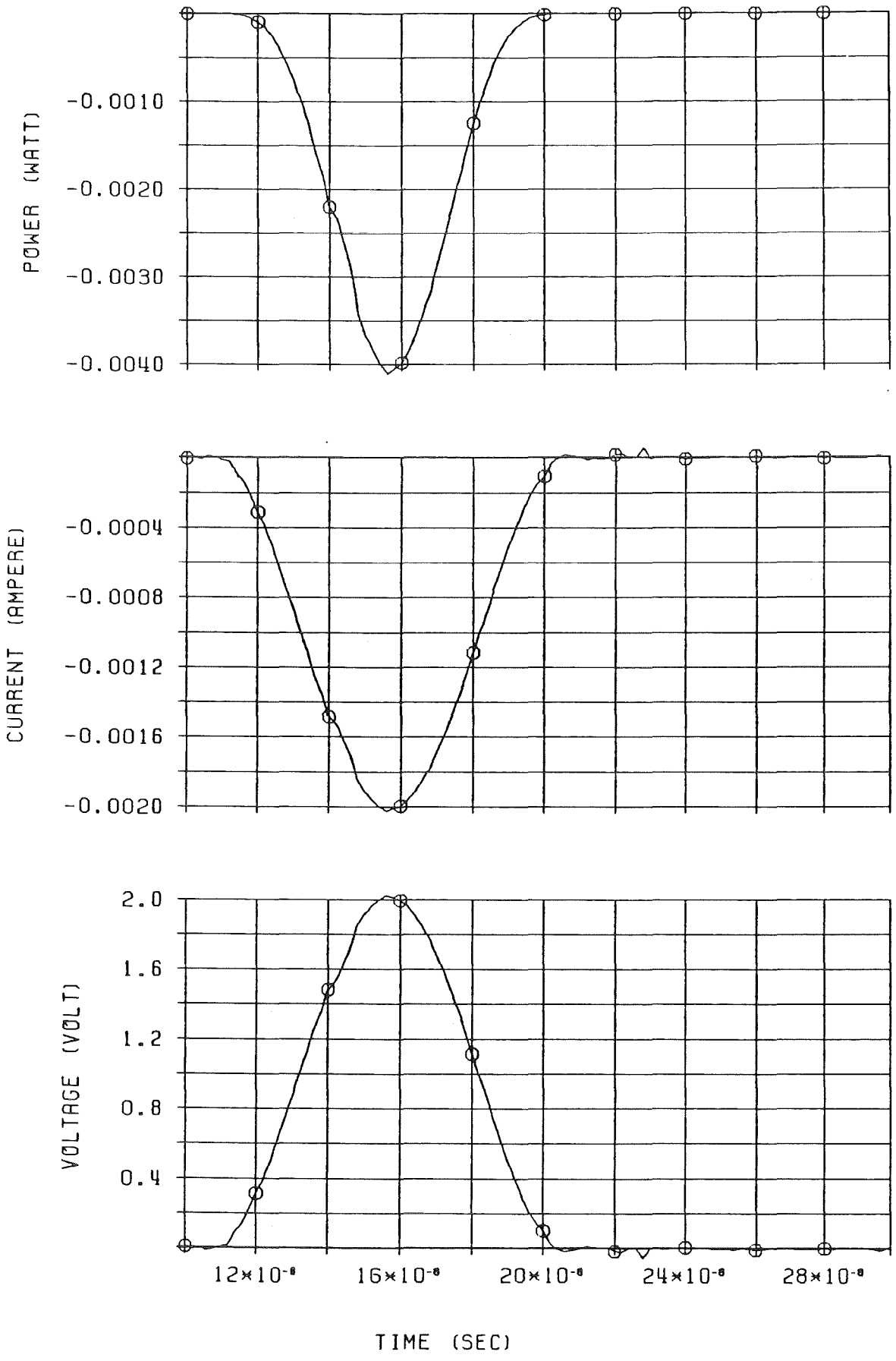

Fig. 12: Voltage enhancement before ignition of the plasma channel caused by large mismatch from a - 1000 Ohm load.

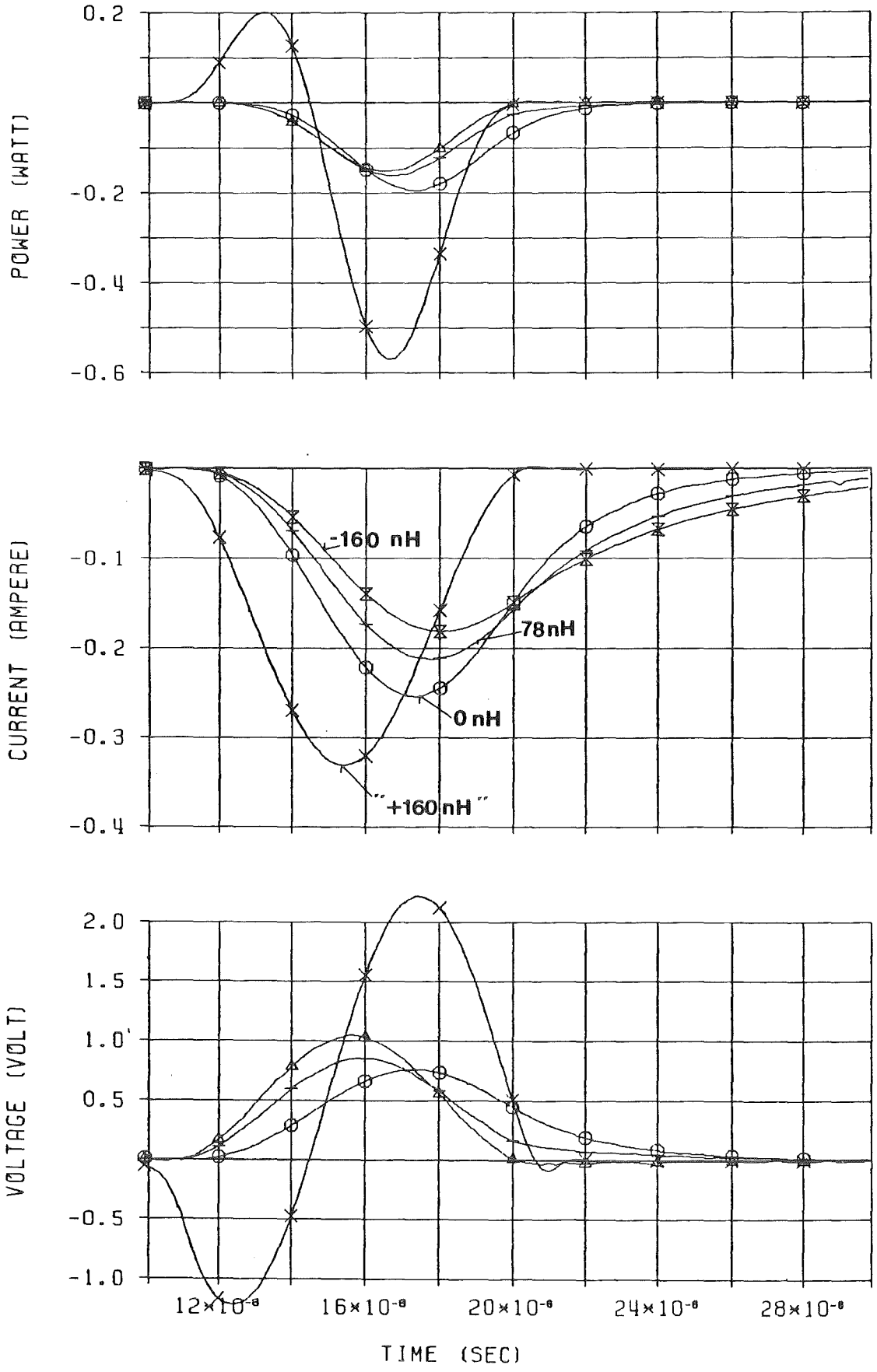

Fig. 13: Influence of a series inductive load of -78 nH and -160 nH relative to an ohmic load (0 nH); the reactive series load "+160nH" mathematically yields the best possible match.

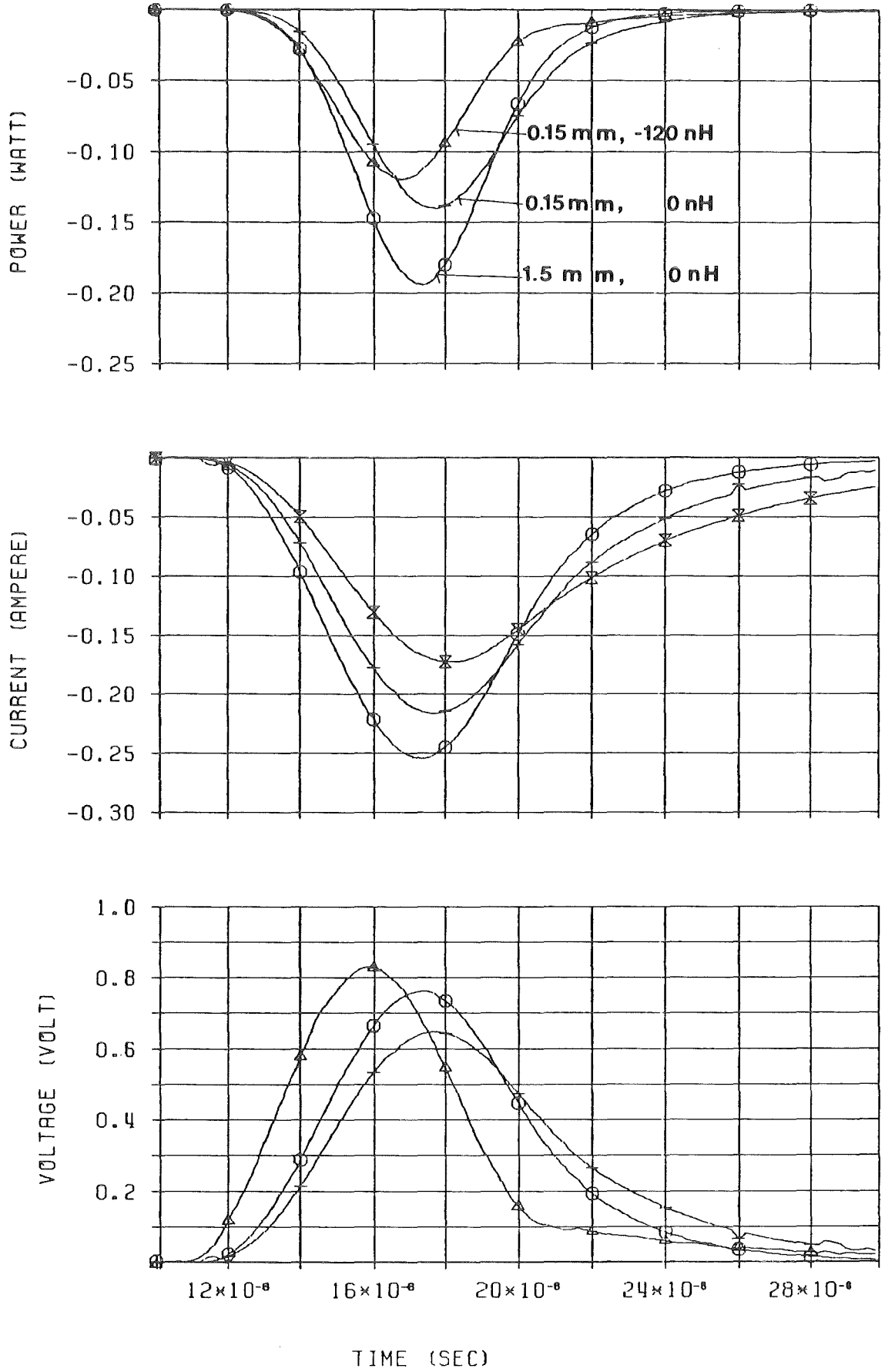

Fig. 14: Influence of load position: comparing two loads at 1.5 mm and 0.15 mm respectively. In one case a -120 nH series inductance is added to the -3 Ohm ohmic load, representing the internal inductance of the plasma channel.

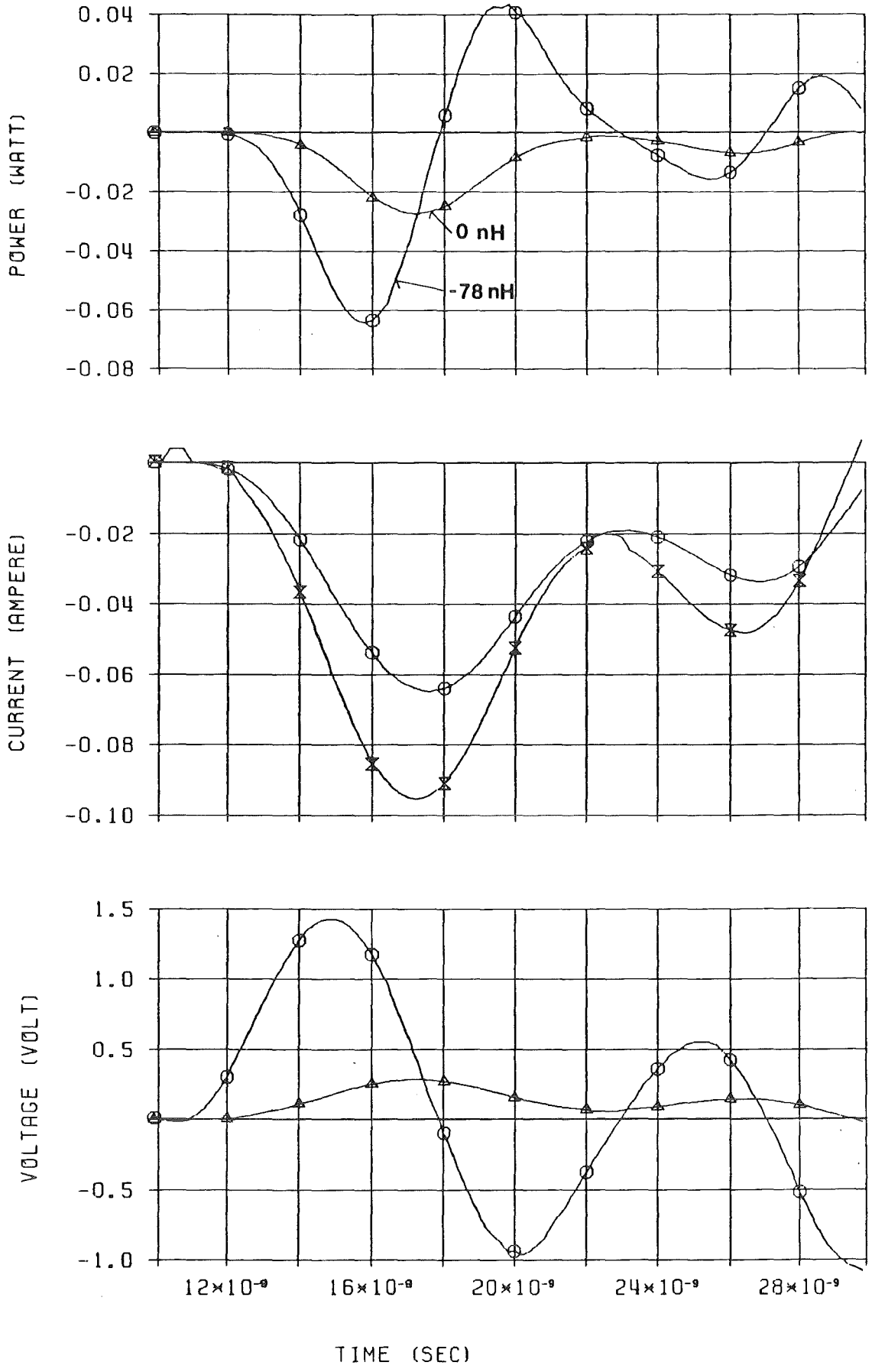

Fig. 15: Influence of high frequency components: 10 ns pulse width at the generator with (-3,0) Ohm and (-3 Ohm, -78 nH) loads.

Appendix

Impedance transformation along a radial line

The impedance transformation along a radial line is mathematically fully described by eq. 27. In this appendix we shall evaluate this impedance transformation for the special case, that the radial line is matched at a radius r_1 for a wave number $k = \sqrt{\varepsilon\mu}\,\omega$ (equ.8). This match is achieved if the impedance at r_1 equals the characteristic impedance of the radial line:

$$\frac{Z(r_1)}{Z_o(r_1)} = 1 \qquad \text{(A1)}$$

Then, taking into account that the characteristic impedance scales inversely proportional to the radius (equ. 23), the relation between the impedance at a radius r to that at the radius r_1 is:

$$\frac{Z(r)}{Z_o(r_1)} = \frac{r_1}{r}\,\frac{C(r,r_1)+j\,s(r,r_1)}{c(r,r_1)+j\,S(r,r_1)} \qquad \text{(A2)}$$

This relation is shown in Fig. 16 for a few values of kr_1 as a function of kr.

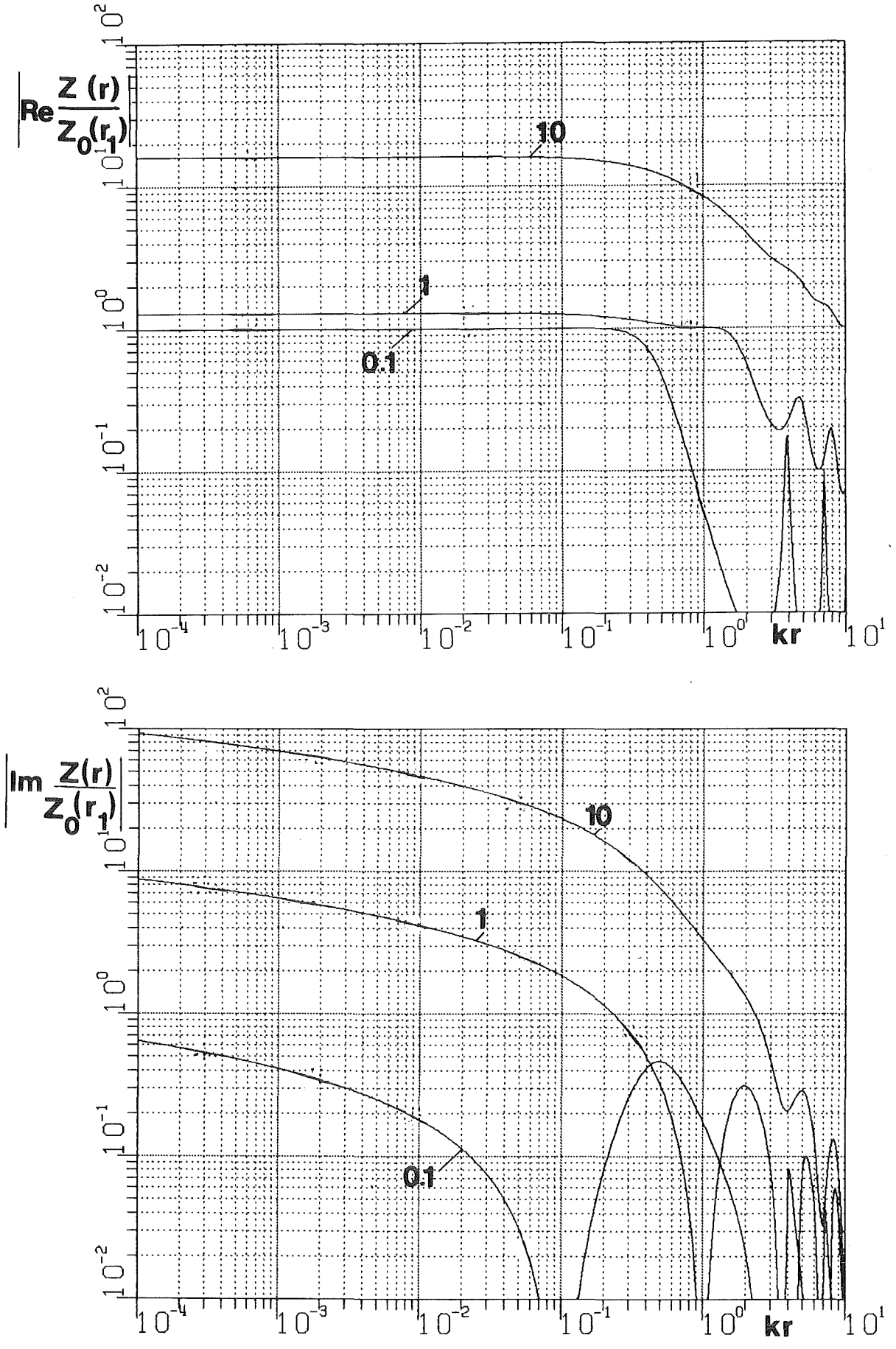

Fig. 16: Impedance of the radial line as a function of the radius r for a fixed wave number k. Parameter is kr_1. The line is matched to its characteristic impedance at the radius r_1.

References

1) M.G. Haines, Physica Scripta, Vol. T2/2, 380 (1982)
2) H. Herold, H.J. Kaeppeler, editors, Proc. of the 3rd Int. Workshop on Plasma Focus Research, Institut für Plasmaforschung der Universität Stuttgart, IPF-83-6 (1983)
3) D. Bloess, I. Kamber, H. Riege, G. Bittner, V. Brückner, J. Christiansen, K. Frank, W. Hartmann, N. Lieser, Ch. Schultheiss, R. Seeböck, W. Stendtner, Nucl. Inst. and Meth. No. 205, 173 (1983)
4) J.A. Nation, Particle Accelerators, Vol. 10, 1 (1979)
5) J.D. Jackson, Classical Electrodynamics, John Wiley & Sons, New York (1967)
6) S. Ramo, J.R. Whinnery, T. van Duzer, Fields and Waves in Communication Electronics John Wiley & Sons, New York (1965)
7) N. Marcuwitz, Radial Transmission Lines, in Principles of Microwave Circuits, C.G. Montgomery, R.H. Dicke, E.M. Purcell, editors, McGraw-Hill Book Comp., New York (1948)
8) N. Marcuwitz, Waveguide Handbook, Mc Graw-Hill Book Comp., New York (1951)